

A. R. Kumar

Z. M. Zhang¹

Department of Mechanical Engineering

V. A. Boychev

D. B. Tanner

Department of Physics
University of Florida,
Gainesville, FL 32611

L. R. Vale

D. A. Rudman

Electromagnetic Technology Division,
National Institute of Standards and Technology,
Boulder, CO 80303

Far-Infrared Transmittance and Reflectance of $\text{YBa}_2\text{Cu}_3\text{O}_{7-\delta}$ Films on Si Substrates

The transmittance and reflectance of superconductive $\text{YBa}_2\text{Cu}_3\text{O}_{7-\delta}$ (YBCO) thin films deposited on Si substrates have been measured in the far-infrared frequency region from 10 to 100 cm^{-1} (wavelength from 1000 to 100 μm) at temperatures between 10 and 300 K. The effects of interference, optical resonance, and antireflection on the radiative properties of high-temperature superconducting (HTSC) films are observed and quantitatively analyzed. Furthermore, we have measured the reflectance of the HTSC film-substrate composites for radiation incident on the substrate side (backside reflectance) for the first time. The backside reflectance increases significantly from the normal state to the superconducting state at certain frequencies; this experimentally demonstrates that HTSC films can be used to build far-infrared intensity modulators. The complex refractive index of the YBCO films is determined from the measured transmittance using the Drude model in the normal state and a two-fluid model in the superconducting state. The complex refractive index obtained from this study is useful for various applications of YBCO films, including radiation modulators, detectors, and Fabry-Perot resonators.

1 Introduction

The radiative properties of high-temperature superconducting (HTSC) films change rapidly from the normal state to the superconducting state in the far-infrared region. This distinguishing characteristic of HTSC films may be used in designing thermooptoelectronic devices such as infrared detectors, intensity and phase modulators, and radiation shields (Zhang and Frenkel, 1994; Zhang, 1998). Additionally, the reflectance of HTSC thin films differs significantly for radiation incident on the substrate side of the film-substrate composite (also called backside illumination) as compared to radiation incident on the film side. Recently, Zhang (1998) presented a design analysis of far-infrared intensity modulators using $\text{YBa}_2\text{Cu}_3\text{O}_{7-\delta}$ (YBCO) films by evaluating the reflectance for various design structures in both the superconducting and normal states. This work predicted large differences in the backside reflectance between the superconducting and normal states. To date, the reflectance of HTSC films has been measured only for radiation incident on the film side (Renk, 1992; Tanner and Timusk, 1992; Zhang et al., 1994). In order to confirm the features associated with the backside illumination, there is a need for measurements of the radiative properties of HTSC films for radiation incident on the substrate.

For the development of HTSC applications, the choice of the substrate material is an important issue. Substrates commonly used for growing HTSC films include MgO , SrTiO_3 , LaAlO_3 , yttria-stabilized zirconia (YSZ), and sapphire (Chen et al., 1995; Phillips, 1996). Several promising far-infrared applications of HTSC films, such as bolometers, modulators, and resonators, demand that the substrate be transparent in the spectral region of interest. Fenner et al. (1993) presented transmittance measurements for various substrates, NdGaO_3 , LaAlO_3 , MgO , YSZ, and Si, in the mid and far-infrared regions. This study showed that the transmittance of Si

is generally higher than that of the other substrates in the measured spectral region. (The transmittance of pure Si is slightly greater than 0.5 at wavelengths longer than 20 μm .) The higher transmittance of Si in a broad spectral region allows new optical designs such as backside-illuminated HTSC microbolometers (Rice et al., 1994). At present, Si substrates have received significant attention from the electronics industry due to the feasibility of lithographically patterning HTSC films and the potential integration of semiconductor and superconducting electronics (Phillips, 1996). High-quality YBCO films have been successfully grown on Si substrates using pulsed laser ablation (Fork et al., 1991; Mechin et al., 1996) but very few measurements have been done to determine the radiative properties of such films. Berberich et al. (1993) measured the transmittance and reflectance of imperfect YBCO films deposited on Si substrates. These films were of poor quality because they were deposited on Si substrates without buffer layers, and the reflectance was measured only at room temperature. Karrai et al. (1992) studied the transmittance of YBCO thin films on Si substrates with and without a magnetic field. However, the substrates were intentionally wedged to avoid interference effects. Most of the reported radiative properties of HTSC superconductors were for opaque samples or thin films on thick substrates (Tanner and Timusk, 1992; Zhang et al., 1994). For transmittance measurements, the interference effects associated with the substrate were often neglected by either averaging over a free spectral range or using wedged substrates (Gao et al., 1991; Karrai et al., 1992; Zhang et al., 1992; Cunsolo et al., 1993). Knowledge of the radiative properties of thin YBCO films deposited on thin substrates is essential for designing optoelectronic devices including radiation modulators and Fabry-Perot resonators (Renk et al., 1990; Genzel et al., 1992; Malone et al., 1993; Zhang, 1998).

The transmittance and reflectance of thin films on transparent substrates typically oscillate periodically as the optical frequency changes, as a result of multiple reflections inside the substrate. This oscillation is particularly prevalent in the far infrared because the wavelength is comparable with the substrate thickness. Hadni et al. (1995) measured the far-infrared transmittance of several YBCO films deposited on MgO substrates. The interference features associated with the substrate were clearly seen in their study

¹ To whom correspondence should be addressed.

Contributed by the Heat Transfer Division for publication in the JOURNAL OF HEAT TRANSFER and presented at 1998 ASME IMECE, Anaheim. Manuscript received by the Heat Transfer Division, Sept. 8, 1998; revision received, May 5, 1999. Keywords: Experimental, Heat Transfer, Interferometry, Radiation, Thin Films. Associate Technical Editor: P. Menguc.

at frequencies from 10 to 40 cm^{-1} . In the present study, several infrared spectrometers have been used to measure both the transmittance and reflectance of YBCO films ($\approx 35\text{-nm}$ thick) deposited on Si substrates ($\approx 200\text{-}\mu\text{m}$ thick), in the frequency region from 10 cm^{-1} to 100 cm^{-1} (wavelength from 1000 to 100 μm) from room temperature down to 10 K. The transmittance was measured with radiation incident on the film side and the reflectance was measured for radiation incident both on the film and on the substrate. The transmittance of the film-substrate composite is the same for radiation incident on the film side and the substrate side. The spectral resolution is chosen high enough to measure the effects of interference associated with the substrate.

Accurate assessments of the potential of YBCO films in optoelectronic applications require the determination of the frequency-dependent radiative properties. Knowledge of the complex dielectric function of the YBCO film facilitates the computation of radiative properties in desired spectral regions (Phelan et al., 1991; 1992). Due to their complicated crystalline structures, the refractive index of the HTSC materials may vary significantly depending on the method of preparation, oxygen content, thickness, and microstructure (Choi et al., 1992; Renk, 1992; Tanner and Timusk, 1992; Flik et al., 1992). In the present study, the measured transmittance spectra are used to determine the complex dielectric function $\epsilon(\omega)$ of YBCO films deposited on Si substrates. In the normal state, a two-component model, consisting of a temperature-dependent free-carrier absorption term (the Drude term) and a temperature-independent mid-infrared term (the Lorentz term), is used for computing $\epsilon(\omega)$. In the superconducting state, the conventional two-fluid model is used for computing $\epsilon(\omega)$ (Tanner and Timusk, 1992). The spectral transmittance and reflectance are calculated with the transfer-matrix method using the refractive indices and thicknesses of the film and the substrate. The dielectric functions are determined at different temperatures by comparing model predictions with measured results. Our measurements demonstrate the feasibility of using thin HTSC films deposited on transparent substrates as radiation modulators. The frequency and temperature-dependent refractive index of the HTSC films obtained from the present study will facilitate future design of potential far-infrared devices based on YBCO films on Si substrates.

2 Experiments

2.1 YBCO Film Preparation. The YBCO films were deposited by pulsed laser ablation using an excimer laser operated at a wavelength of 248 nm. A single-crystal (100) Si wafer, polished on both sides with a thickness of approximately 200 μm and a diameter of 76 mm, was used as the substrate. The wafer is slightly boron-doped and has an electric resistivity of $\approx 1000\ \Omega\text{-cm}$. The Si wafer, was cut into approximately $12 \times 12\ \text{mm}^2$ pieces for the deposition of the YBCO. Ag paste was used to mount the substrate onto a substrate holder in the deposition chamber. At high temperatures, Ag may diffuse into the Si substrate. Therefore, a 320-nm thick SiO_2 layer was deposited by chemical vapor depo-

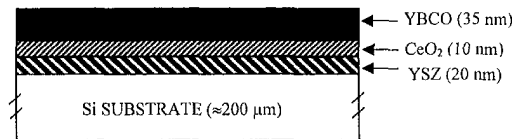


Fig. 1 Structure of the film-substrate composite (the lateral dimensions are $\approx 12 \times 12\ \text{mm}^2$)

sition (CVD) on the backside of the Si substrate before the application of the Ag paste. The substrate was heated to 1063 K for the deposition of a 20-nm thick YSZ layer and then a 10-nm thick CeO_2 layer on the Si substrate. These buffer layers are required for growing high-quality superconducting films (Mechin et al., 1996). A YBCO film of 35 nm was deposited on the top of the buffer layers at 1043 K in an optimized O_2 environment (Rice et al., 1994). The thicknesses of the thin films were determined by calibrations of the rate of deposition. The YBCO films formed this way are a - b plane oriented (c -axis is parallel to the surface normal) with a critical temperature (T_c) between 86 and 88 K.

Several steps were followed to remove the Ag paste and the SiO_2 layer. First, the YBCO film was covered by a photoresist. Second, nitric acid (HNO_3) was used to remove Ag paste and then hydrofluoric acid (HF) was used to etch off the SiO_2 layer. Third, the photoresist was removed using acetone. Finally the film was rinsed with isopropanol. The structure of the film is shown in Fig. 1. Some damage to the film may have taken place during this stripping process since the critical temperature of several films dropped to 80 to 82 K after the removal of the photoresist. However, scanning electron microscopic (SEM) images showed no evidence of microcracks or other surface damage.

2.2 Transmittance and Reflection Measurements. The transmittance spectra of the films were measured using a slow-scan Michelson interferometer with a Hg-arc lamp as the source (Gao, 1992). The entire interferometer chamber is evacuated to eliminate the absorption by atmospheric gases. The source radiation is modulated by a rotating chopper inside the chamber to allow lock-in detection. This procedure allows only in-phase modulated radiation to be detected and thus minimizes the effect of external noise. The radiation is guided by mirrors and light pipes to the sample and thence to the detector. Polyethylene windows, which are transparent in the far-infrared region, are used to seal the cryostat. The detection system consists of a 4.2 K He-cooled Si bolometer. A preamplifier and lock-in electronics are used to measure the detector output signal.

The sample holder consists of two identical copper plates with equally sized apertures in the middle. The copper plates are mounted at a right angle. One aperture is covered by the specimen and the other is left blank for the reference measurement. The sample holder is mounted on the cold finger of the cryostat. The cold finger is kept in high vacuum and cooled by flowing liquid He

Nomenclature

c_0 = speed of light in vacuum, $2.9979 \times 10^8\ \text{m/s}$
 d = thickness, m
 f_s = fraction of superconducting electrons
 $i = (-1)^{1/2}$
 k = imaginary part of refractive index
 N = complex refractive index
 n = real part of the refractive index
 n_e = electron number density, m^{-3}
 r = reflection coefficient
 T = transmittance
 T_c = critical temperature, K

y = dimensionless admittance of the film
 δ = phase change
 $\Delta\omega$ = free spectral range, m^{-1}
 γ_e = damping constant in the Lorentz term, rad/s ; ($1\ \text{rad/s} = 5.3089 \times 10^{-12}\ \text{cm}^{-1}$)
 ϵ = dielectric function
 ϵ_0 = electric permittivity of free space, $8.8542 \times 10^{-12}\ \text{C} \cdot \text{V}^{-1} \cdot \text{m}^{-1}$
 ϵ_∞ = high-frequency dielectric constant
 λ = wavelength in vacuum, m

$1/\tau$ = electron scattering rate, rad/s
 σ_{DC} = DC conductivity, $(\Omega \cdot \text{m})^{-1}$
 ω = angular frequency, rad/s
 ω_c = center frequency, rad/s
 ω_p = plasma frequency, rad/s
 ω_{pe} = plasma frequency in the Lorentz term, rad/s

Subscripts

f = film
 Si = silicon

at 4.2 K, which results in conductive cooling of the specimen. A diffusion pump is used to achieve a vacuum of 10^{-2} Pa inside the cryostat before cooling; the actual pressure should be much lower due to cryopumping. The liquid He is transferred from a liquid-helium tank via an evacuated transfer line. The specimen temperature is measured using a Si diode. An automatic temperature controller was used to adjust the temperature of the specimen using a proportional-integral-derivative (PID) control scheme and an electric heater wrapped around the cold finger. The temperature variation was within 0.5 K of the set temperature for measurements above 100 K. During the measurements at 10 K and 50 K, the variation of temperature was about 1 K from the set temperature.

The cryostat, along with the sample holder, is introduced vertically into the interferometer chamber. The cryostat can be rotated so that either the blank aperture or the specimen is in the beam path of the far-infrared radiation. For the transmittance measurement, the spectrum obtained with the blank is taken as the background spectrum. The cryostat is then rotated by 90 degrees to introduce the specimen in the beam path. The exact position of the cryostat for the blank aperture or for the specimen is determined by gently rotating the cryostat until the signal is maximum. The transmitted spectrum of the specimen is divided by the background spectrum to obtain the transmittance. The spectral resolution is approximately 0.5 cm^{-1} .

The reflectance was measured using a commercial fast-scan Fourier transform spectrometer. The spectrum is averaged over 128 scans and the resolution is $\approx 1 \text{ cm}^{-1}$. Here, the far-infrared beam is directed to either the specimen or a Au mirror by a combination of plane and elliptical mirrors. The angle of incidence in the reflectance measurement is $\approx 7.5^\circ$ with a beam divergence of 7.5° . The Au mirror is used as the reference for the reflectance measurements at all temperatures. In the far-infrared region, the reflectance of the gold is greater than 0.995 at room temperature and increases at lower temperatures. Hence, the reflectivity of the Au mirror is taken to be 1.

The transmittance and reflectance of bare Si substrates were measured at different temperatures to evaluate the measurement uncertainty. The refractive index of single-crystal Si has been well documented (Loewenstein et al., 1973). The use of the high-resistivity single-crystal Si has essentially eliminated absorption in the substrate. The measured transmittance shows interference patterns with T_{\max} about 1, T_{\min} about 0.3, and a free spectral range $\Delta\omega$ (the wave number interval between two interference maxima) about 7 cm^{-1} . Even a small variation in the substrate thickness (d_{Si}) or its refractive index (n_{Si}) can affect $\Delta\omega$, since $\Delta\omega = (2n_{\text{Si}}d_{\text{Si}})^{-1}$. The Si thickness is determined from the free spectral range by assuming that $n_{\text{Si}} = 3.42$ at frequencies from 10 to 100 cm^{-1} (Loewenstein et al., 1973). The actual angles of incidence in the transmittance measurement have a spread up to 18 degrees as a result of the beam divergence in the light pipe. The effect of inclined incidence on $\Delta\omega$ (and hence d_{Si}) is less than 0.5 percent since the angle of refraction inside the silicon is small. The transmittance extrema shift toward higher frequencies as the temperature decreases, indicating a decrease of the refractive index since the thickness change can be neglected (Loewenstein et al., 1973). The measured transmittance is compared with the calculated transmittance to determine the refractive index at different temperatures. The results are $n_{\text{Si}} \approx 3.405$ at 200 K, 3.395 at 100 K, and 3.39 at 50 K and 10 K. For the same Si wafer, the transmittance maxima become the reflectance minima at all temperatures.

Although the interference patterns in the measured transmittance and reflectance of the Si substrate match theoretical predictions, the radiometric accuracy is not as high. The maximum transmittance often varies between 0.95 and 1.05 or more near the spectral cutoffs. The reflectance minimum is always greater than zero, which may be caused by the insufficient spectral resolution. The root-mean-square difference between the measured and the calculated values shows a standard uncertainty of ≈ 0.05 in both the transmittance and reflectance. Hence, the expanded uncertainty (95 percent confidence) is estimated to be 0.1 for all measure-

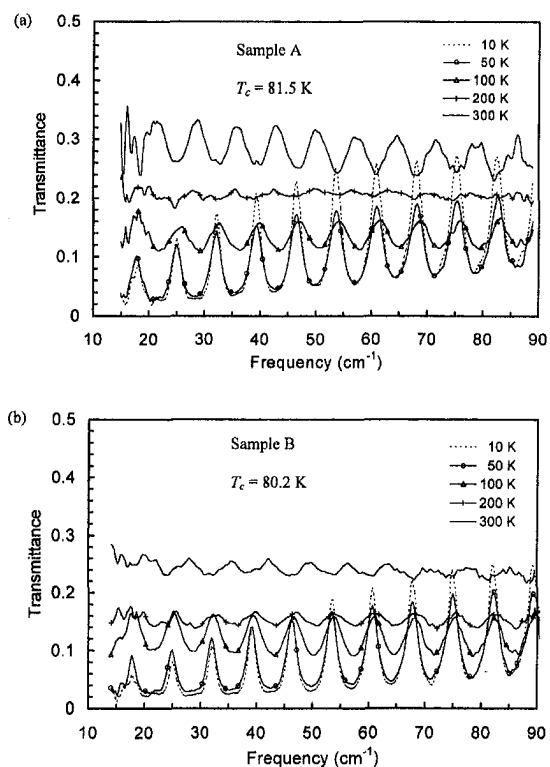


Fig. 2 Measured transmittance of YBCO films on Si substrates at various temperatures

ments. This uncertainty is large compared with the measurements without sharp interference fringes, which could be caused by many parameters, such as detector nonlinearity, misalignment, phase error, and multiple reflections between the sample, windows, and the beam splitter (Griffiths and de Haseth, 1986; Zhang et al., 1996).

Figure 2 shows the measured transmittance of two specimens, identified as Sample A and Sample B, at various temperatures. The transmittance spectra oscillate periodically due to interference effects inside the substrate with $\Delta\omega$ slightly higher than 7 cm^{-1} . In the normal state, the fringe-averaged transmittance, defined as $\bar{T}(\omega) = (1/\Delta\omega) \int_{\omega-\Delta\omega/2}^{\omega+\Delta\omega/2} T(\omega') d\omega'$, is nearly uniform for all the measured frequencies at any given temperature but decreases gradually as the temperature is lowered. This decrease is expected because the electrical conductivity of the YBCO film increases as temperature decreases. The interference pattern is quite periodic over the studied wave number range at any given temperature, but varies significantly as the temperature is changed from 300 K to 100 K. Not only do the peak locations vary with temperature but also the fringe contrast (the relative amplitude of oscillation) changes significantly. There is a phase shift of π rad between the 300 K and 100 K data; that is, the transmittance maxima at one temperature correspond to the transmittance minima at the other. Furthermore, the spectrum at 200 K for Sample A has no discernible interference fringes, which can be attributed to an antireflection effect of the YBCO film. In the superconducting state, the fringe-averaged transmittance is lower at smaller frequencies and increases toward higher frequencies. The peak transmittance is higher at lower temperatures. This is caused by the optical resonance effect in the film-substrate composite and by decreasing losses in the film. The antireflection effect on the interference pattern at 200 K and the effect of optical resonance on the peak transmittance in the superconducting state are discussed in Section 5.

The measured reflectance spectra of Sample A are shown in Fig. 3 for radiation incident on the substrate. The fringe-averaged

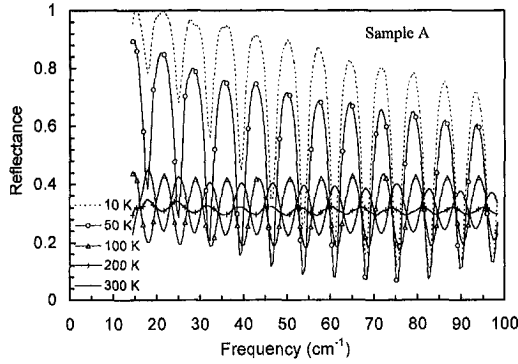


Fig. 3 Measured reflectance for radiation incident on the substrate (backside)

reflectance is nearly independent of wave number in the normal state, but increases toward smaller frequencies in the superconducting state. The reflectance increases sharply as the temperature is reduced to below the critical temperature and increases slightly as the temperature is further reduced. The fringe contrast is much higher in the superconducting state than in the normal state. In a way similar to the transmittance, the fringe contrast is much smaller at 200 K than at 300 K and 100 K. At frequencies where the transmittance is maximum, the reflectance for radiation incident on the substrate decreases to minimum values. The large change in the reflectance of YBCO films at particular frequencies, from the superconducting to the normal state, experimentally demonstrate that HTSC films can be used to construct far-infrared intensity modulators as proposed by Zhang (1998).

Using suitable dielectric function models, the complex refractive index of the YBCO film is determined by fitting the measured transmittance data because the transmittance measurement has a better spectral resolution, which is especially important in the region where sharp interference extrema occur. Comparison is also made between the calculated and measured reflectance whenever the data are available. Detailed discussions are given below.

3 Analysis

3.1 Dielectric Function Models for the Superconductor YBCO. The optical properties of superconducting YBCO change abruptly from the normal state to the superconducting state. Hence, different dielectric function models are used in the normal and superconducting states (Tanner and Timusk, 1992). In the normal state, the frequency-dependent complex dielectric function can be modeled as a sum of the Drude term (ϵ_{Drude}), the Lorentz term ($\epsilon_{\text{Lorentz}}$), and a high-frequency constant ($\epsilon_{\infty} \approx 5$):

$$\epsilon(\omega) = \epsilon_{\text{Drude}} + \epsilon_{\text{Lorentz}} + \epsilon_{\infty}. \quad (1)$$

The Drude term describes the electronic behavior in the infrared region by assuming that free electrons (or holes) are accelerated in the presence of an electric field and that collisions result in a damping force. Thus, the Drude term can be expressed as

$$\epsilon_{\text{Drude}} = -\frac{\omega_p^2}{\omega(\omega + i/\tau)} \quad (2)$$

where ω is the angular frequency, ω_p is the plasma frequency, and $1/\tau$ is the electron scattering rate. The plasma frequency is defined as $\omega_p^2 = n_e e^2 / m \epsilon_0$, where n_e , e , and m are the electron number density, charge, and effective mass, and ϵ_0 is the electric permittivity of free space. The plasma frequency, the scattering rate, and the DC electrical conductivity σ_{DC} are related by

$$\omega_p^2 = \frac{\sigma_{\text{DC}}}{\epsilon_0 \tau}. \quad (3)$$

From Eqs. (2) and (3), only σ_{DC} and $1/\tau$ are needed to calculate ϵ_{Drude} .

The Lorentz term can be derived by assuming that the electrons are bound to their nuclei by harmonic forces and are subjected to damping forces. Lorentz terms are also commonly used to model infrared active phonons. The phonon contributions, however, can be neglected compared to the electronic contributions (Choi et al., 1992). This neglect is particularly valid in the far infrared because the resonant frequencies of most phonons are in the mid-infrared region. For HTSC materials, however, there is a broadband mid-infrared electronic absorption, which is typically modeled with a Lorentz term (Tanner and Timusk, 1992). This contribution is therefore expressed as

$$\epsilon_{\text{Lorentz}} = \frac{\omega_{pe}^2}{\omega_e^2 - \omega^2 - i\omega\gamma_e} \quad (4)$$

where ω_{pe} , ω_e , and γ_e are, respectively, the plasma frequency, center frequency, and damping constant of the mid-infrared band. Due to the relatively weak effect of the Lorentz term in the far infrared, a single oscillator is used with the parameters fixed to those recommended by Zhang et al. (1994), i.e., $\omega_e = 1800 \text{ cm}^{-1}$, $\omega_{pe} = 18000 \text{ cm}^{-1}$, and $\gamma_e = 5400 \text{ cm}^{-1}$. The effect of the mid-infrared band on the radiative properties of the film is very weak at frequencies between 10 and 100 cm^{-1} , because $\epsilon_{\text{Lorentz}}$ is essentially a real constant, $\approx (\omega_{pe}/\omega_e)^2$ in the far infrared. Calculations using different Lorentz parameters, such as $\omega_e = 1800 \text{ cm}^{-1}$, $\omega_{pe} = 24150 \text{ cm}^{-1}$, $\gamma_e = 7500 \text{ cm}^{-1}$ (Flik et al., 1992), do not modify significantly the transmittance and reflectance of the film-substrate composite.

Below the critical temperature T_c , the free-carrier part of the dielectric function is described by a two-fluid model. In this model, only a fraction of electrons (f_s) are assumed to be in the condensed phase (or superconducting state) and the remaining electrons are in the normal state. The superconducting electrons move without any scattering, and the value of f_s is assumed temperature-dependent. The contribution of the superconducting electrons to the dielectric function is

$$\epsilon_{\text{sup}} = -\frac{\omega_p^2}{\omega^2}. \quad (5)$$

The Drude term remains due to the presence of normal electrons with a number density of $(1 - f_s)n_e$. The dielectric function in the superconducting state is therefore modeled as

$$\epsilon(\omega) = f_s \epsilon_{\text{sup}} + (1 - f_s) \epsilon_{\text{Drude}} + \epsilon_{\text{Lorentz}} + \epsilon_{\infty}. \quad (6)$$

3.2 Fitting Procedure. The transfer-matrix method, described by Zhang and Flik (1993), is used to compute the transmittance and reflectance of the film-substrate composite shown in Fig. 1. The Si substrate is assumed to be nonabsorbing and to have the temperature-dependent refractive index described in Section 2.2. The effective thickness of the Si substrate is determined by matching the interference patterns between the calculated and measured spectra. The angle of incidence has little effect except for a slight shift in the frequencies of the interference fringes, which has already been accounted for using the effective thickness of the Si substrate. Hence, the angle of incidence is assumed to be normal in all calculations.

The absorption of dielectric materials, such as YSZ and CeO_2 , is very weak in the far-infrared region, especially for thickness less than 20 nm. The dielectric constant of YSZ is 25 and that of CeO_2 is 17 in the far-infrared and microwave regions (Grishchowsky and Keiding, 1990; Phillips, 1996). In all cases, the addition of the YSZ and CeO_2 layers has essentially no effect on the calculated transmittance and reflectance. Therefore, the YSZ and CeO_2 layers are omitted in the calculations and not discussed further.

The real part $n_r(\omega)$ and imaginary part $k_f(\omega)$ of the complex refractive index of the YBCO film are related to the dielectric function by

Table 1 Fitting parameters, where the expanded uncertainties are estimated to be ten percent in $1/\sigma_{DC}$, 20 percent in $1/\tau$, and 20 percent in f_s

	Sample A ($T_c = 81.5$)			Sample B ($T_c = 80.2$)		
Temp. (K)	$1/\sigma_{DC}$ ($\mu\Omega\text{-cm}$)	f_s	$1/\tau$ (cm^{-1})	$1/\sigma_{DC}$ ($\mu\Omega\text{-cm}$)	f_s	$1/\tau$ (cm^{-1})
300	800	-	600	700	-	600
200	538	-	400	460	-	440
100	306	-	230	290	-	275
50	-	0.25	150	-	0.30	180
10	-	0.35	190	-	0.40	220

$$(n_f + ik_f)^2 = \epsilon(\omega) \quad (7)$$

where $\epsilon(\omega)$ is calculated from Eq. (1) and Eq. (6) for the normal and superconducting states, respectively. The refractive index of YBCO is used to calculate the transmittance and reflectance of the film-substrate composite.

In the normal state, σ_{DC} and $1/\tau$ are taken as adjustable parameters. Their values are determined by fitting the calculated transmittance to the measured transmittance. The best fit is obtained when the root-mean-square difference is the smallest. In some cases, the differences in the fringe-averaged transmittance and the peak transmittance are also used to determine the best fit when the root-mean-square difference is not so sensitive to the parameters. Our calculations show that the radiative properties depend strongly on σ_{DC} but weakly on $1/\tau$, suggesting a larger uncertainty in $1/\tau$. The fitted values of σ_{DC} and $1/\tau$ at room temperature are used to compute the plasma frequency from Eq. (3). The plasma frequency is proportional to the total electron density and is typically constant over temperature (Kamarás et al., 1990; Tanner and Timusk, 1992). Hence, at other temperatures in the normal state, the scattering rate is the only adjustable parameter. Both the superconducting-electron fraction f_s and the scattering rate $1/\tau$ are considered to be adjustable parameters in computing the dielectric function of YBCO in the superconducting state.

4 Results

The fitting parameters for both specimens are shown in Table 1 (Kumar, 1999). The difference in the fitted values may be caused by the slight variation in the film deposition conditions. Figure 4 compares the fitted and measured transmittance of Sample A. The fitted and measured values agree well with a root-mean-square difference of less than 0.03 in most cases. At temperatures greater than T_c , both the scattering rate and the resistivity drop almost linearly with decreasing temperature. At these temperatures, the scattering rate is dominated by the temperature-dependent electronic scattering, which governs the linear dependence of resistivity on the temperature. At low temperatures, below T_c , the temperature-dependent scattering ceases to exist, and the remaining scattering is mainly due to impurities and lattice defects, which should be temperature-independent (Flik et al., 1992). This scattering rate should be constant at low temperatures. However, the best agreement between the measured and calculated transmittance at 10 K was achieved with a scattering rate higher than that for 50 K. This unexpected higher scattering rate at lower temperatures needs further investigation, although it could simply be caused by the experimental uncertainty. Bonn et al. (1992) showed that the scattering rate of YBCO decreases drastically as the temperature is reduced below T_c , due to the rapid reduction of the density of thermally activated quasi-particles. Their results, however, were

for a single-crystal $\text{YBa}_2\text{Cu}_3\text{O}_7$ of extremely high quality with $f_s \approx 1$ at very low temperatures.

Even at very low temperatures, there is a large fraction $(1 - f_s)$ of normal-state electrons in the thin YBCO films. For conventional superconductors, f_s should be zero at temperatures much lower than T_c . The definition of f_s for HTSC materials is rather ambiguous. Some researchers obtained higher values of f_s by assuming that a portion of the YBCO film is not superconductive, also known as "dead layer" (Renk, 1992; Hadni et al., 1995). In the present study, the superconducting fraction is calculated without assuming any dead layer, and this may account for the small values of f_s obtained in this study. Another reason may be the higher DC resistivity ($1/\sigma_{DC}$) of our YBCO films in the normal state. The DC resistivity is strongly affected by the choice of the substrate and buffer layers, by their thicknesses, as well as by the thickness of the YBCO film (Mechin et al., 1996). The damage caused by the stripping process as mentioned in Section 2.1 may have reduced f_s as well. Although the critical temperature of Sample A is slightly higher than that of sample B, the fraction of superconducting electrons of Sample A is less than that of sample B. This may be explained by the fact that Sample A has a higher electrical resistivity and scattering rate.

The real and imaginary parts of the refractive index of YBCO calculated from Eq. (7) using the fitting parameters for Sample A are shown in Fig. 5. Both n_f and k_f increase as the wave number decreases at all temperatures. In the normal state, $n_f \approx k_f$, as

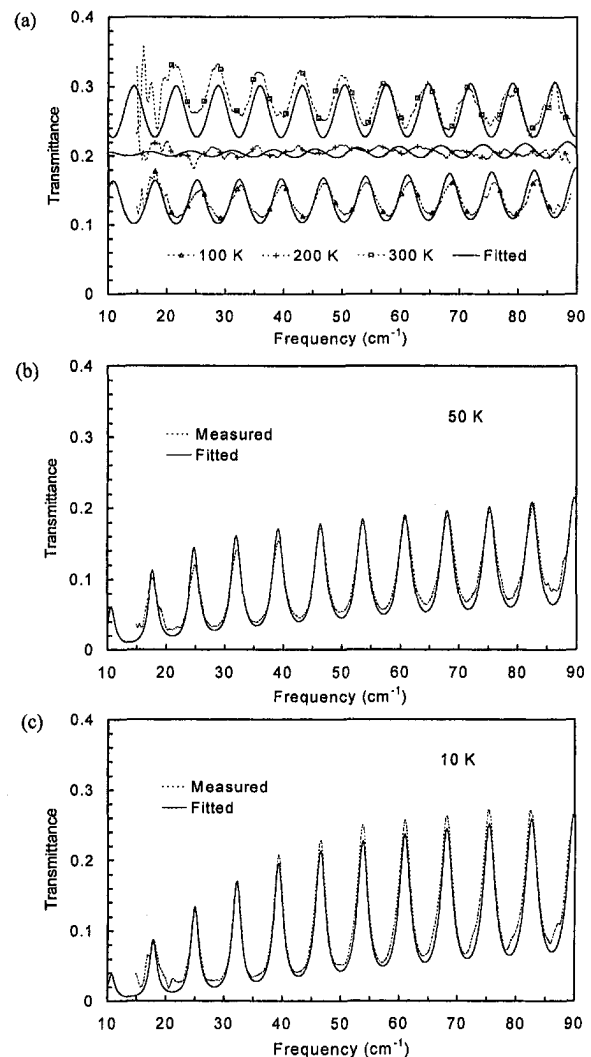


Fig. 4 Comparison between the measured and fitted transmittance for Sample A: (a) normal state; (b) 50 K; (c) 10 K

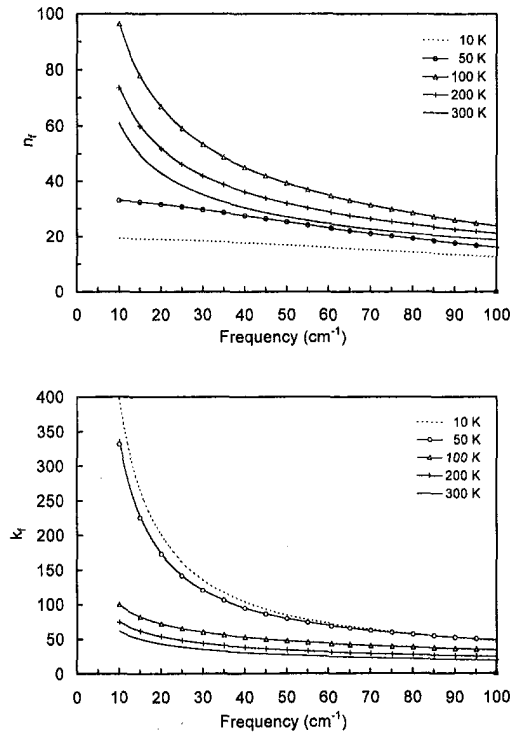


Fig. 5 Complex refractive index of the YBCO film (Sample A)

expected for a metallic film, and both n_f and k_f increase with decreasing temperature. As the film becomes superconducting, n_f drops suddenly but k_f exhibits an abrupt increase, especially at low frequencies. As the temperature is further reduced from 50 K to 10 K, n_f continues to decrease whereas k_f continues to increase. Below T_c , $k_f \gg n_f$, because the film is largely inductive in its optical response. The refractive index of Sample B has a similar trend (Kumar, 1999), but now in the superconducting state the imaginary part is even greater and the real part is even smaller due to a slightly larger fraction of superconducting electrons (see Table 1). The expanded uncertainty in the real and imaginary parts of the refractive index is estimated to be ten percent.

Figure 6 compares the measured with the calculated reflectance at 50 K and 10 K for radiation incident on the substrate. The measured and calculated reflectance is in reasonable agreement. At the reflectance minima, the calculated values are much lower than those measured, which may be caused by insufficient resolution in the measured reflectance or by the beam divergence. Further improvements in radiometric accuracy and spectral resolution are required in order to resolve the discrepancy between the measured and calculated reflectance.

5 Discussion

5.1 The Antireflection Effect. For Sample A, measurements reveal that the minima in the transmittance at 300 K approximately correspond to the maxima at 100 K, 50 K, and 10 K (see Fig. 2(a)). The measured transmittance at 200 K has no discernible interference fringes. This interesting change in the interference pattern is analyzed below by considering the radiation incident from the substrate and reflected by the film. The reflection coefficient at the substrate-film interface is the ratio of the reflected to the incident electric waves (Heavens, 1965):

$$r = \frac{-r_{23} + r_{21}e^{i2\delta_f}}{1 - r_{23}r_{21}e^{i2\delta_f}} \quad (8)$$

where, for normal incidence, $r_{21} = (N_2 - N_1)/(N_2 + N_1)$ and $r_{23} = (N_2 - N_3)/(N_2 + N_3)$, and $\delta_f = \omega d_f N_2 / c_0$ is the complex

phase change in the film. Note that $N_1 = 1$, $N_2 = N_f$, and $N_3 = n_{\text{Si}}$ correspond to the refractive indices of the air, film, and the substrate, respectively, and c_0 is speed of light in vacuum. If $|2i\delta_f| \ll 1$, which is satisfied for the thin YBCO film in the normal state, then $\exp(2i\delta_f) \approx 1 + 2i\delta_f$. The requirement of $|2i\delta_f| \ll 1$ is equivalent to (1) $d_f \ll \lambda/4\pi k_f$ (the film thickness is much smaller than the radiation penetration depth), where λ is the wavelength in vacuum, and (2) $d_f \ll \lambda/4\pi n_f$. After some manipulation, Eq. (8) becomes

$$r \approx \frac{N_3 - N_1 + i\delta_f N_2(1 + N_3/N_2)(1 - N_1/N_2)}{N_3 + N_1 - i\delta_f N_2(1 - N_3/N_2)(1 - N_1/N_2)} \quad (9)$$

Assume $|N_1/N_2| \ll 1$ and $|N_3/N_2| \ll 1$, which are also valid since the refractive index and extinction coefficient of metallic films (such as YBCO in the normal state) are generally much greater than the refractive index of dielectric materials (such as the Si substrate used here). Then,

$$r \approx \frac{N_3 - N_1 + i\delta_f N_2}{N_3 + N_1 - i\delta_f N_2} \quad (10)$$

Equation (10) is the same as that derived by McKnight et al. (1987), but here it is obtained directly from Maxwell's equations without assuming that the film is infinitely thin. It is convenient to define a dimensionless admittance, $y = -i\delta_f(N_f)$, which in general is a complex quantity. As discussed above, the dielectric function of YBCO in the normal state is dominated by the Drude term, which becomes purely imaginary at frequencies much smaller than the scattering rate ($\omega\tau \ll 1$); hence, $\epsilon(\omega) \approx i\sigma_{\text{DC}}/\omega\epsilon_0$. From the definitions of y and δ_f , $y \approx \sigma_{\text{DC}}d_f/c_0\epsilon_0$ is a real positive constant in the very far infrared. When $y = n_{\text{Si}} - 1$, the reflection coefficient given by Eq. (10) becomes zero for incidence on the substrate. For $N_3 = n_{\text{Si}} \approx 3.4$, the required DC resistivity ($1/\sigma_{\text{DC}}$) is $\approx 550 \mu\Omega\text{-cm}$ for $d_f = 35 \text{ nm}$. The DC resistivity obtained by fitting the transmittance at 200 K of $538 \mu\Omega\text{-cm}$ is very close to

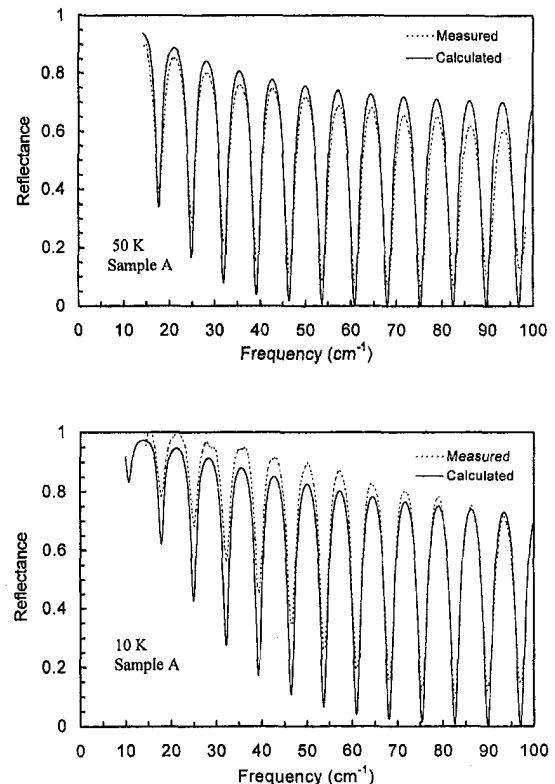


Fig. 6 Measured and calculated backside reflectance for Sample A at 50 K and 10 K

this value. However, because the scattering rate is only 400 cm^{-1} at 200 K (see Table 1), there are residual interference fringes. Because of all the assumptions made earlier, interference fringes persist in the calculated transmittance even with $1/\sigma_{\text{DC}} \approx 550 \mu\Omega\text{-cm}$. McKnight et al. (1987) analyzed and experimentally demonstrated the effect of antireflection coating (also called impedance-matched coating) on the transmittance of a Si wafer coated with a Ni-Cr film. In that work, the scattering rate was much greater than 100 cm^{-1} , and the fringe contrast in the measured transmittance was much smaller.

The change from transmittance maxima at 300 K to transmittance minima at 100 K at fixed wave number can be explained by the sign change of the reflection coefficient given by Eq. (10) as the DC resistivity passes $\approx 550 \mu\Omega\text{-cm}$. The change in the sign of this coefficient, combined with the interference effect inside the Si substrate, will result in a phase shift of π rad in the interference pattern and thus causing the transmittance to change from maxima to minima and vice versa. The calculated transmittance and reflectance agree extremely well in terms of the interference patterns at all temperatures except for Sample A at 200 K. The actual phase at 200 K is very complicated because the assumptions used in deriving Eq. (10) are not perfectly met. The discrepancy in the phase between the calculated and the measured transmittance at 200 K suggests that the scattering rate is complex and may depend on the wave number. Modified Drude models with a complex and frequency-dependent scattering rate have been used for the study of HTSC materials (Varma et al., 1989; Virosztek and Ruvalds 1990; Renk, 1992; Quinlan et al., 1996). Further studies are needed to investigate the applicability of these models to thin YBCO films on Si substrates.

The fringe patterns of Sample B differs from those of Sample A, because their characteristics are different. From Fig. 2(b) and Table 1, we can estimate that the interference contrast for Sample B would be the smallest at a temperature somewhere between 300 K and 200 K, where its DC electric resistivity is near $550 \mu\Omega\text{-cm}$. The condition for impedance matching with the Si substrate is that $(\sigma_{\text{DC}}d_f)^{-1} \approx 157 \Omega$. Hence, it is possible to construct antireflection coatings with a YBCO film on Si substrate at room temperature by increasing the film thickness. The practical applications of the antireflection effect using HTSC films need further exploration.

5.2 The Effect of Optical Resonance. The measured spectra for both specimens at 10 K and 50 K have sharper transmittance maxima and reflectance minima than the spectra obtained above the critical temperature (see Figs. 2 and 3). In addition, the peak transmittance at 10 K is even higher than that at 50 K. The transmittance is expected to decrease as the temperature is lowered since the YBCO material becomes more and more conductive. The unexpected higher transmittance at lower temperatures in certain spectral bands is the result of optical resonance in the film-substrate composite. A simple optical resonator is a dielectric layer coated with highly reflecting films on both sides. By varying the reflection coefficient of one or both coatings, the transmittance of the resonator can be altered significantly. This resonance effect will result in very high transmittance values at particular frequencies (Klein and Furtak, 1986). In the present study, the specimen is analogous to an optical resonator made of a thin YBCO film coated on only one side of the Si substrate. As the temperature is reduced to below the critical temperature, the reflection coefficient of the YBCO film increases sharply. The large reflection coefficient, coupled with the interference effects in the substrate, can significantly increase the measured transmittance at certain frequencies. The observed resonance effects demonstrate that YBCO films deposited on Si substrates have the potential for construction of Fabry-Perot resonators (Renk et al., 1990; Genzel et al., 1992; Malone et al., 1993). Further studies are needed to construct resonance structures using two identical films facing each other to optimize the performance of such resonators. The calculated minimum transmittance is slightly lower at 10 K than at 50 K. This is consistent with the measured values for Sample B. The measured

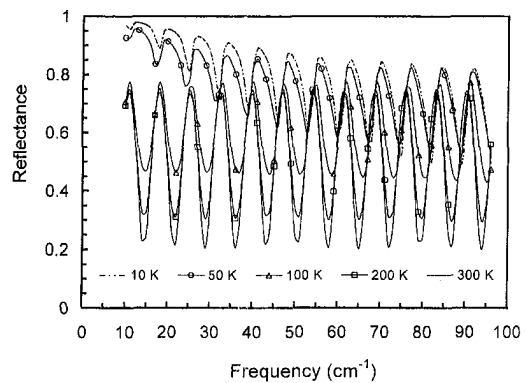


Fig. 7 Calculated film side reflectance for Sample A

minimum transmittance for Sample A is nearly the same at 10 K and 50 K at large frequencies. However, the expected difference is smaller than the experimental uncertainty.

5.3 The Film Side Reflectance. The film side reflectance for Sample A is calculated using the fitted parameters and is shown in Fig. 7. In the normal state, the peak locations of the interference fringes remain at the same frequency. The film side reflectance shows a higher fringe contrast in the normal state and a lower fringe contrast in the superconducting state when compared to the substrate side reflectance. The reflectance measurements on several sample films for the film side incidence agree well with the above-mentioned pattern (Kumar, 1999).

6 Conclusions

We have measured the transmittance and reflectance of thin YBCO films deposited on transparent Si substrates in the far-infrared region at temperatures from 10 K to 300 K. The measurements show fringes caused by interference effects within the Si substrate. The change in the DC conductivity of the YBCO film with temperature causes a change in the reflection coefficient at the substrate-film interface, which results in a variation of the interference pattern. Matching of the admittance of the YBCO film with the refractive index of the Si substrate will yield a zero reflection coefficient at the substrate-film interface and thus eliminate the fringes in the measured transmittance. A change in the sign of the reflection coefficient results in a phase change of π rad in the interference pattern.

Sharp increases in the transmittance maxima in the superconducting state indicate that optical resonance has occurred within the film-substrate composite. The reflectance for radiation incident on the substrate increases significantly upon switching from the normal state to the superconducting state. These phenomena demonstrate that the HTSC thin films on transparent substrates can be used to build far-infrared devices, such as optical resonators and radiation modulators.

The transmittance and reflectance are calculated using the Drude model in the normal state and the two-fluid model in the superconducting state. The predicted values agree closely with the measured values using only a few adjustable parameters. The complex refractive index of the YBCO films is thus obtained at different temperatures. The imaginary part increases steeply as the superconducting state is reached but the real part shows a sudden decrease. The refractive index of YBCO films obtained from this study is important for the design of promising devices using HTSC thin films. Future research is needed to improve the quality of the YBCO films on Si substrates as well as the reproducibility of the deposition process. Methods for improving the radiometric accuracy in the spectrometric measurements with sharp interference fringes need to be further investigated.

Acknowledgments

This research was partially supported by the University of Florida through an Interdisciplinary Research Initiative (IRI) award, and the National Science Foundation through grants DMR-9705108 and CTS-9812027.

References

- Berberich, B., Chiusuri, M., Cunsolo, S., Dore, P., Kinder, H., and Varsamis, C. P., 1993, "Far-Infrared Spectra of Imperfect YBaCuO Films on Si Substrates," *Infrared Physics*, Vol. 34, pp. 269–279.
- Bonn, D. A., Dosanjh, P., Liang, R., and Hardy, W. N., 1992, "Evidence for Rapid Suppression of Quasiparticle Scattering below T_c in YBa₂Cu₃O_{7.8}," *Phys. Rev. Lett.*, Vol. 68, pp. 2390–2393.
- Chen, R. C., Wu, J. P., and Chu, H. S., 1995, "Bolometric Response of High- T_c Superconducting Detectors to Optical Pulses and Continuous Waves," *ASME JOURNAL OF HEAT TRANSFER*, Vol. 117, pp. 366–372.
- Choi, B. C., Zhang, Z. M., Flik, M. I., and Siegrist, T., 1992, "Radiative Properties of Y-Ba-Cu-O Films With Variable Oxygen Content," *ASME JOURNAL OF HEAT TRANSFER*, Vol. 114, pp. 958–964.
- Cunsolo, S., Dore, P., Lupi, S., Trippetti, R., Varsamis, C. P., and Sherman, A., 1993, "Infrared Conductivity of YBCO from Transmittance and Reflectance Spectra of Thin Films," *Physica C*, Vol. 211, pp. 22–28.
- Fenner, D. B., Li, Q., Hamblen, W. D., Johansson, M. E., Hamblen, D. G., and Lynds, L., 1993, "Optical and Thermal Performance Advantages for Silicon Substrates in YBCO Bolometer Devices," *IEEE Trans. Appl. Supercond.*, Vol. 3, pp. 2104–2106.
- Flik, M. I., Zhang, Z. M., Goodson, K. E., Siegal, M. P., and Phillips, J. M., 1992, "Electron Scattering Rate in Epitaxial YBa₂Cu₃O₇ Superconducting Films," *Phys. Rev. B*, Vol. 46, pp. 5606–5614.
- Fork, D. K., Fenner, D. B., Barrera, A., Phillips, J. M., Geballe, T. H., Connell, G. A. N., and Boyce, J. B., 1991, "Buffer Layers for High-Quality Epitaxial YBCO Films on Si," *IEEE Trans. Appl. Supercond.*, Vol. 1, pp. 67–73.
- Gao, F., Carr, G. L., Porter, C. D., Tanner, D. B., Etemad, S., Venkatesan, T., Inam, A., Dutta, B., Wu, X. D., Williams, G. P., and Hirschmugl, C. J., 1991, "Far-Infrared Transmittance and Reflectance Studies of Oriented Thin Films," *Phys. Rev. B*, Vol. 43, pp. 10,383–10,389.
- Gao, F., 1992, "Temperature Dependence of Infrared and Optical Properties of High Temperature Superconductors," Ph.D. dissertation, Department of Physics, University of Florida, Gainesville, FL.
- Genzel, I., Bauer, M., Yoder, R., and Habermeyer, H.-U., 1992, "Far-Infrared Investigations on YBa₂Cu₃O₇ Films with the Use of a Reflection Fabry-Perot Interferometer," *Solid State Communications*, Vol. 81, pp. 589–592.
- Griffiths, P. R., and de Haseth, J., 1986, *Fourier Transform Infrared Spectrometry*, John Wiley and Sons, New York, Chapter 1.
- Grischkowsky, D., and Keiding, S., 1990, "THz Time-Domain Spectroscopy of High T_c Substrates," *Appl. Phys. Lett.*, Vol. 57, pp. 1055–1057.
- Hadni, A., Gerbaux, X., Cudraz, H. M., Tazawa, M., Mage, J. C., Marcilhac, B., Mercandalli, and Mansart, D., 1995, "Residual Losses of Superconducting Thin Films of YBa₂Cu₃O_{7.8} in the Far Infrared and Microwaves: Applications," *Physica C*, Vol. 245, pp. 219–230.
- Heavens, O. S., 1965, *Optical Properties of Thin Solid Films*, Dover, New York, Chapter 4.
- Kamarás, K., Herr, S. L., Porter, C. D., Tache, N., Tanner, D. B., Etemad, S., Venkatesan, T., Chase, E., Inam, A., Wu, X. D., Hegde, M. S., and Dutta, B., 1990, "In a Clean High- T_c Superconductor You Do Not See the Gap," *Phys. Rev. Lett.*, Vol. 64, pp. 84–87.
- Karrai, K., Choi, E., Dunmore, F., Liu, S., Ying, X., Li, Q., Venkatesan, T., Drew, H. D., Li, Q., and Fenner, D. B., 1992, "Far-Infrared Magneto-Optical Activity in Type-II Superconductors," *Phys. Rev. Lett.*, Vol. 69, pp. 355–358.
- Klein, M. V., and Furtak, T. E., 1986, *Optics*, 2nd Ed., John Wiley and Sons, New York, Chapter 5.
- Kumar, A. R., 1999, "Far-Infrared Radiative Properties of Superconducting YBCO Films Deposited on Silicon Substrates," Ph.D. dissertation, Department of Mechanical Engineering, University of Florida, Gainesville, FL.
- Loewenstein, E. V., Smith, D. R., and Morgan, R. L., 1973, "Optical Constants of Far-Infrared Materials, 2: Crystalline Solids," *Appl. Opt.*, Vol. 12, pp. 398–406.
- Malone, C. G., Zhang, Z. M., Flik, M. I., and Cravalho, E. G., 1993, "Optimized Design of Far-Infrared Fabry-Perot Resonators Fabricated from YBa₂Cu₃O₇," *IEEE Trans. Appl. Supercond.*, Vol. 3, pp. 2852–2855.
- Mechin, L., Villegier, J. C., Rolland, G., and Laugier, F., 1996, "Double CeO₂/YSZ Buffer Layer for the Epitaxial Growth of YBa₂Cu₃O_{7.8} Films on Si (001) Substrates," *Physica C*, Vol. 269, pp. 124–130.
- McKnight, S. W., Stewart, K. P., Drew, H. D., and Moorjani, K., 1987, "Wavelength-Independent Anti-Interference Coating for the Far-Infrared," *Infrared Physics*, Vol. 27, pp. 327–333.
- Phelan, P. E., Flik, M. I., and Tien, C. L., 1991, "Radiative Properties of Superconducting Y-Ba-Cu-O Thin Films," *ASME JOURNAL OF HEAT TRANSFER*, Vol. 113, pp. 487–493.
- Phelan, P. E., Chen, G., and Tien, C. L., 1992, "Thickness-Dependent Radiative Properties of Y-Ba-Cu-O Thin Films," *ASME JOURNAL OF HEAT TRANSFER*, Vol. 114, pp. 227–233.
- Phillips, J. M., 1996, "Substrate Selection for High-Temperature Superconducting Thin Films," *Journal of Applied Physics*, Vol. 79, pp. 1829–1848.
- Quinlan, S. M., Hirschfeld, P. J., and Scalapino, D. J., 1996, "Infrared Conductivity of $d_{x^2-y^2}$ -Wave Superconductor with Impurity and Spin-Fluctuation Scattering," *Phys. Rev. B*, Vol. 53, pp. 8575–8582.
- Renk, K. F., Betz, J., Schützmann, J., Prückl, A., Brunner, B., and Lengfellner, H., 1990, "Use of High T_c Superconductors for Far-Infrared Fabry-Perot Resonators," *Appl. Phys. Lett.*, Vol. 57, pp. 2148–2149.
- Renk, K. F., 1992, "Far-Infrared Spectroscopy of High Temperature Superconductors," *Studies of High Temperature Superconductors*, A. V. Narlikar, ed., Nova Science Publishers, New York, Vol. 10, pp. 25–62.
- Rice, J. P., Grossman, E. N., and Rudman, D. A., 1994, "Antenna-Coupled High- T_c Air-Bridge Microbolometer on Silicon," *Appl. Phys. Lett.*, Vol. 65, pp. 773–775.
- Tanner, D. B., and Timusk, T., 1992, "Optical Properties of High-Temperature Superconductors," *Physical Properties of High-Temperature Superconductors*, D. M. Ginsberg, ed., World Scientific Publishing Co., Singapore, Vol. 3, pp. 363–469.
- Varma, C. M., Littlewood, P. B., Schmitt-Rink, S., Abrahams, E., and Ruckenstein, A. E., 1989, "Phenomenology of the Normal State of Cu-O High-Temperature Superconductors," *Phys. Rev. Lett.*, Vol. 63, pp. 1996–1999.
- Virosztek, A., and Ruvalds, J., 1990, "Nested-Fermi-Liquid Theory," *Phys. Rev. B*, Vol. 42, pp. 4064–4072.
- Zhang, Z. M., Choi, B. I., Le, T. A., Flik, M. I., Siegel, M. P., and Phillips, J. M., 1992, "Infrared Refractive Index of Thin YBa₂Cu₃O₇ Superconducting Films," *ASME JOURNAL OF HEAT TRANSFER*, Vol. 114, pp. 644–652.
- Zhang, Z. M., and Flik, M. I., 1993, "Predicted Absorptance of YBa₂Cu₃O₇/YSZ/Si Multilayer Structures for Infrared Detectors," *IEEE Trans. Appl. Supercond.*, Vol. 3, pp. 1604–1607.
- Zhang, Z. M., and Frenkel, A., 1994, "Thermal and Nonequilibrium Responses of Superconductors for Radiation Detectors," *Journal of Superconductivity*, Vol. 7, pp. 871–884.
- Zhang, Z. M., Le, T. A., Flik, M. I., and Cravalho, E. G., 1994, "Infrared Optical Constants of the High- T_c Superconductor YBa₂Cu₃O₇," *ASME JOURNAL OF HEAT TRANSFER*, Vol. 116, pp. 253–257.
- Zhang, Z. M., Hanssen, L. M., Datla, R. U., and Drew, H. D., 1996, "An Apparatus for Infrared Transmittance and Reflectance Measurements at Cryogenic Temperatures," *International Journal of Thermophysics*, Vol. 17, pp. 1441–1454.
- Zhang, Z. M., 1998, "Far-Infrared Radiation Modulators Using High- T_c Superconductors," *ASME JOURNAL OF HEAT TRANSFER*, Vol. 120, pp. 24–29.